Prediction of cure-induced spring-in of an angle bracket

This example demonstrates the use of multiscale technology combined with cure modeling in Abaqus/Standard to model the cure-induced spring-in deformation of an angle bracket.

This example demonstrates the following Abaqus features and techniques:

- composite cure modeling in Abaqus/Standard;
- a viscoelasticity model with thermorheologically simple dependence on temperature and degree of cure;
- the use of a multiscale material model to homogenize thermal, chemical, and mechanical properties;
- a fully coupled thermal-displacement procedure to model the transient response of the composite during curing; and
- the model change technique to remove contact definitions for spring-in deformation prediction.

In addition, it compares the fully coupled approach with a sequentially coupled approach.

This page discusses:

- Application description
- Abaqus modeling approaches and simulation techniques
- Input files
- References
- Tables
- Figures

Products: Abaqus/Standard

Application description

Composite cure process–induced shape distortion presents significant challenges in composite products manufacturing. Cure process simulation requires the modeling of thermal, chemical, and mechanical responses of the composite material. During the curing process, the manufacturer-recommended heating cycle is applied to the composite part. The degree of cure of the composite increases with time, and this evolution is characterized by the cure kinetics of the process. Residual stress/strain can develop with the change of thermal/chemical condition, leading to shape distortion once the composite part is separated from the mold/tool.

Geometry

The geometry of the angle bracket assembly has two main components: the composite angle bracket and the steel tool. Figure 1 shows the dimensions of the cross-section of the L-shaped bracket. The width of the bracket is 60 cm. The bracket has a $(0/90)_n$ layup. The width of the tool is 80 cm, with a thickness of 50 cm. Figure 2 shows the bracket-tool assembly.

Boundary conditions and loading

During the curing simulation, the bottom surfaces of the tool are fixed in all directions. Film conditions are applied to all exterior surfaces. The film coefficient is set to 60 W/m^{2}K for the top of the bracket and the tool. The film coefficient for the side and bottom of the tool is set to 30 W/m^{2}K. Figure 3 shows the temperature applied during the curing cycle.

Abaqus modeling approaches and simulation techniques

Two modeling approaches are used in this example:

- Fully coupled temperature-displacement analysis.
- Sequentially coupled analysis. A heat-transfer analysis is performed first to predict the temperature change in the composite. A quasi-static analysis is then performed using the temperature history imported from the heat-transfer analysis.

Mesh design

C3D8T elements are used in the fully coupled analysis. In the sequentially coupled analysis, DC3D8 elements are used in the heat-transfer analysis and C3D8 elements are used in the subsequent mechanical analyses. There are 10 layers of elements in the thickness direction.

Materials

The tool is made of steel, with properties as listed in Table 1. The bracket material is modeled with LY5052 epoxy reinforced with 55% E-glass fiber. Table 2 lists the properties of the E-glass, which are based on those in Table 1.

The cure characteristics of LY5052 are based on those in Saseendran and Wysocki (2016). The Kamal definition is used for the cure kinetics, and the standard DiBenedetto equation is used to compute the glass transition temperature from the degree of cure. Table 3 and Table 4 list the Kamal coefficients and the parameters in the DiBenedetto equation, respectively. Another important aspect of the cure reaction is that a considerable amount of energy can be released during curing, which can result in exothermal temperature peaks and drastic changes in temperature and degree of cure. The cure heat generation is set to 4.82e5 J/Kg (Saseendran and Wysocki (2016)).

During the curing process, the cure temperature in the resin changes with time. With this change, the resin material undergoes two transformations. The first one is a transformation from a liquid to a solid, which is called gelation. At this point, the material is in a rubbery state. As the glass transition temperature increases and eventually exceeds the cure temperature, the material transforms from a rubbery state to a glassy state. This second transformation is called vitrification. Table 5 and Table 6 list the properties of the resin at the glassy state and the rubbery state.

The mechanical constitutive relationship of the resin material can be modeled as linear viscoelastic with thermorheologically simple effects. For simplicity, a simple shift function proposed by Svanverg (2002) is used:

$$A = \lim_{\omega \to 0} \begin{cases} \omega, T \geq T_g \\ \frac{1}{\omega}, T < T_g \end{cases}.$$

With this simplified shift function (see Temperature Effects), the resin material reaches full relaxation instantaneously in the rubbery state and has no relaxation once it reaches the glassy state. In the shift function definition, 10^{-20} is used for the rubbery state and 10^{35} is used for the glassy state. The relaxation of the modulus is adapted from Prony series coefficients in Kim and White (1996).

During the curing process, the resin material undergoes permanent shrinkage due to the cross-linking reaction. Cure shrinkage, thermal strain, and residual stresses developed during the curing process are the main contributing factors to the shape distortion of the composite part after tool removal. The thermal strain in this example is modeled in the following rate:

$$\dot{\epsilon}^{th} = \alpha \dot{\theta},$$

in which α is the thermal expansion coefficient given by

$$\alpha = \begin{cases} \alpha^r, T \geq T_g \\ \alpha^g, T < T_g \end{cases},$$

in which α^r and α^g are, respectively, the thermal expansion coefficient of the rubbery state and the glassy state. The thermal expansion coefficient is assumed to be zero before gelation—the degree of cure is less than 0.5. Two approaches are used to model the thermal expansion: one is through user subroutine UEXPAN, and the other is through a tabular tangent definition (see Thermal Expansion). The cure shrinkage is modeled with a similar rate formulation (see Cure Shrinkage Strain).

Two approaches are demonstrated to model the local fiber directions. In the first approach, the composite is modeled as a unidirectional fiber-reinforced composite , and the local fiber direction is specified in the 1- and 2-direction in alternate layers of the mesh. In the second approach, the composite is modeled with a single woven material, which contains two inclusions that are orthogonal to each other.

Initial conditions

The initial temperature of both the bracket and the tool is 22°C. The initial degree of cure of the resin in the composite is 0.001.

Interactions

During the analysis the normal interaction between the bracket and tool is specified as "hard" contact with no separation. Rough friction is specified to describe the interaction in the tangential direction during the mechanical analysis. Node-to-surface contact is specified to ensure that all nodes on the bottom surface of the bracket stay attached to the tool. In the last step, contact between the bracket and the tool is removed.

Analysis steps

The fully coupled analysis consists of two steps. The first step is a coupled temperature-displacement step, in which the temperature shown in Figure 3 is applied to the exterior of the bracket and tool to simulate the cure process. The second step is also a coupled temperature-displacement step, in which contact between the bracket and the tool is removed. The bracket continues to cool to room temperature during this step, and shape distortion of the bracket is evaluated under the free-standing condition.

The sequentially coupled analysis consists of three steps. The first step is a heat-transfer step, in which the temperature shown in Figure 3 is applied to the exterior of the bracket and tool to simulate the cure process. The second step is a quasi-static step, in which the temperature history from the heat-transfer step is imported. Thermal expansion, cure shrinkage, and residual stresses are predicted in this step. The third step is a static step, in which contact between the bracket and the tool is removed and shape distortion of the bracket is evaluated under a "free-standing" condition. For efficiency, room temperature is prescribed, and the bracket reaches equilibrium in a single increment.

Results and discussion

The time history of the temperature, degree of cure, and glass transition temperature evaluated at one of the corner elements of the bracket is shown in Figure 4. The part temperature is close to the applied temperature with little exothermic overshoot. Figure 5 and Figure 6 show the temperature distribution in the whole assembly predicted by the two approaches (fully coupled and sequentially coupled). Little temperature gradient over the assembly is observed, which validates the proper choice of the tool material. The difference in results between the fully coupled and sequentially coupled approaches is very small, indicating insignificant effect of deformation on the change of temperature and degree of cure.

For the case when the bracket is modeled with alternate layers of UD composite, the final shape distortion results are shown in Figure 7 and Figure 8. The deformed shape of the bracket is overlaid on the undeformed shape. The amplitude of the deformation is amplified five times. The predicted spring-in angle predicted by both approaches is approximately 1°, which is close to the prediction by Svanverg (2002). The displacements of the top corner node predicted by both approaches are shown in Figure 10, and the predictions are very close. The in-plane strains (E11, CURESE11, THE11) and out-of-plane strains (E22, CURESE22, THE22) predicted by the sequential analysis are shown in Figure 11 and Figure 12. Due to the unconstrained condition at the top of the bracket, the strains in the thickness direction are significant larger than the in-plane strains. The strains predicted by the fully coupled analysis are very close to the prediction of the sequentially coupled

analysis. Figure 13 shows the in-plane (S11) and out-of-plane (S22) residual stresses predicted by both approaches. Most of the residual stresses developed after the composite transforms from the rubbery state to the glassy state.

For the case when the bracket is modeled with a woven composite, the final shape distortion result is shown in Figure 9. The analysis is fully coupled. The spring-in angle predicted is close to the prediction given by the UDcomposite.

Input files

anglebracket3d_composite.inp

Fully coupled temperature-displacement model (UD definition).

anglebracket3d_composite_heat.inp

Heat-transfer model in the sequentially coupled analysis (UD definition).

anglebracket3d_composite_mech.inp

Subsequent quasi-static model in the sequentially coupled analysis (UD definition).

anglebracket3d_woven_composite.inp

Fully coupled temperature-displacement model (woven definition).

anglebracket_material.inp

Input file containing material definition of the composite material (UD definition). Thermal expansion coefficient is specified with user subroutine UEXPAN.

anglebracket_woven_material.inp

Material definition for the composite material (woven definition). The thermal expansion coefficient is specified with user subroutine UEXPAN.

anglebracket_material_tangent.inp

Material definition for the composite material (UD definition). The thermal expansion coefficient is specified with the tangent definition.

uexpan_cureconst.f

User subroutine UEXPAN.

References

Svanverg, J., "Shape Distortion of Non-Isothermally Cured Composite Angle Bracket," *Plastics, Rubber and Composites*, vol. 31, pp. 398–404, 2002.

Saseendran, S., M. Wysocki, and J. Varna, "Evolution of Viscoelastic Behavior of a Curing LY5052 Epoxy Resin in the Glassy State," *Advanced Manufacturing: Polymer & Composites*

Science, vol. 2, pp. 74–82, 2016.

Saseendran, S., , and M. Wysocki, "Characterisation of Viscoelastic Material Properties during Curing Process," *Challenges in Mechanics of Time-Dependent Materials*, vol. 2, pp. 45–54, 2016.

Kim, Y., and S. White, "Stress Relaxation Behavior of 3501-6 Epoxy Resin during Cure," *Polymer Engineering Science*, vol. 36, no. 23, pp. 2852–2862, 1996.

Tables

Table 1. Tool properties.

Young's modulus (GPa)	193
Poisson's ratio	0.29
Density (kg/m^3)	8000
Thermal expansion coefficient (K^{-1})	1.73×10^{-5}
Conductivity (W/m/K)	16.2
Specific heat (J/kg/K)	420

Table 2. Fiber properties.

Young's modulus (GPa)	76
Poisson's ratio	0.22
Density (kg/m^3)	2540
Thermal expansion coefficient (K^{-1})	4.9×10^{-6}
Conductivity (W/m/K)	1.0
Specific heat (J/kg/K)	800

Table 3. Kamal model coefficients.

Z (1/sec)	274906.7
E (J/mol)	54888.35
m	0.25
n	1.01
b	0.0

Table 4. Parameters in the DiBenedetto equation.

T_{g0} (K)	232.15
$T_{g\infty}$ (K)	409.15
λ	0.44

Table 5. Properties of resin (glassy state).

Bulk modulus (GPa)	3.6
Shear modulus (GPa)	0.94
Thermal expansion coefficient (K^{-1})	71×10^{-6}

Table 6. Properties of resin (rubbery state).

Bulk modulus (GPa)	3.6
Shear modulus (GPa)	0.0094
Thermal expansion coefficient (K^{-1})	178×10^{-6}

Table 7. Other resin properties.

Density (kg/m^3)	1100
Conductivity (W/m/K)	0.3
Specific heat (J/kg/K)	$3.0\theta + 51.9$
Cure shrinkage coefficient	−0.018

Figures

Figure 1. Dimensions of the cross-section of the angle bracket.

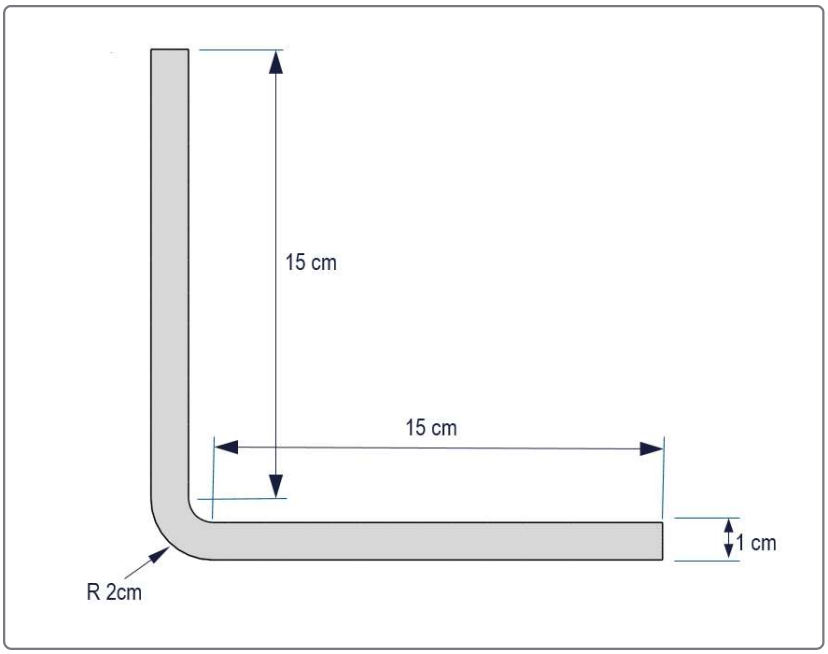

Figure 2. Bracket-tool assembly.

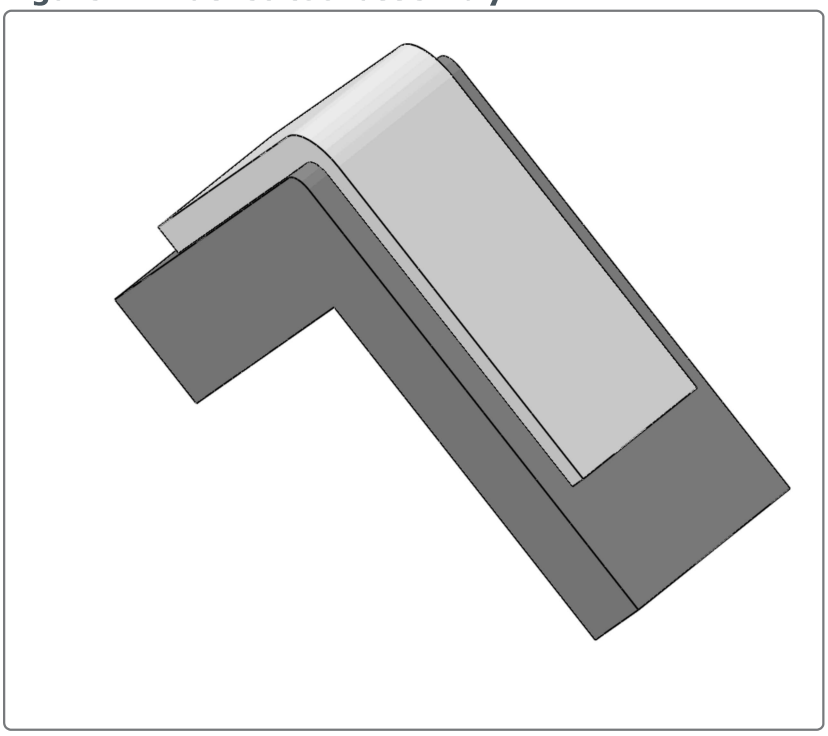

Figure 3. Applied temperature.

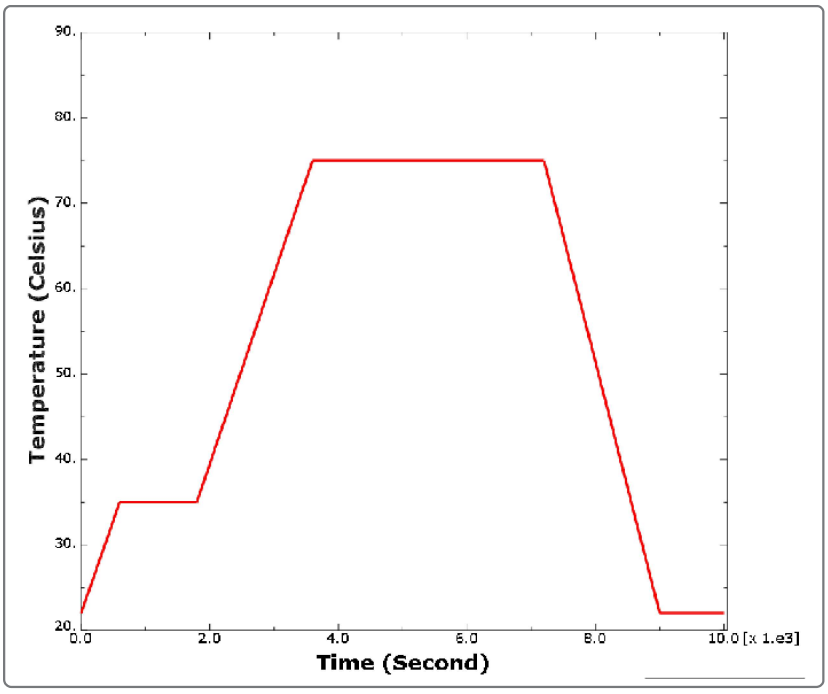

Figure 4. Time history of the temperature, degree of cure and glass transition temperature.

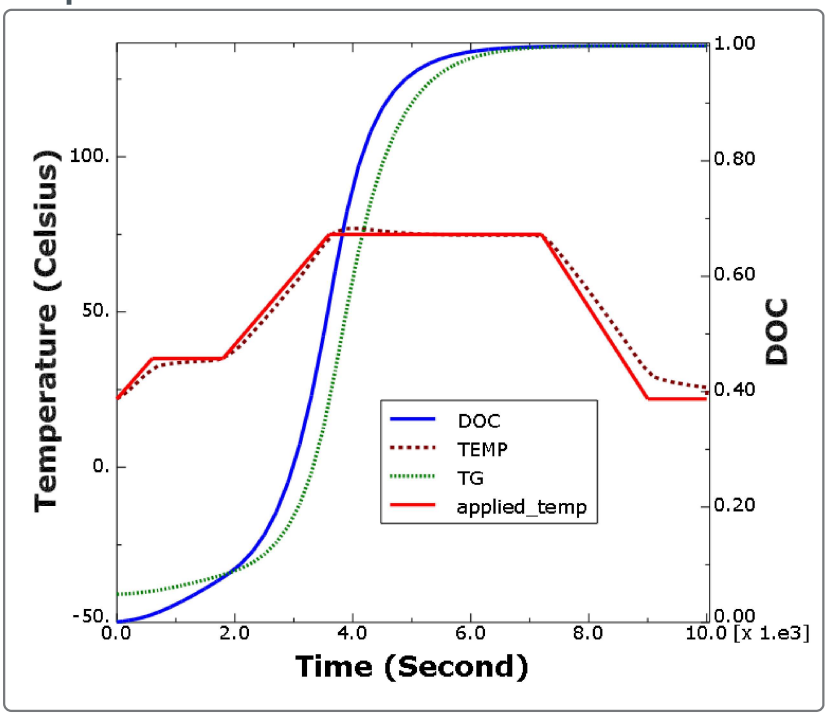

Figure 5. Temperature distribution of the bracket and tool assembly predicted by the fully coupled analysis.

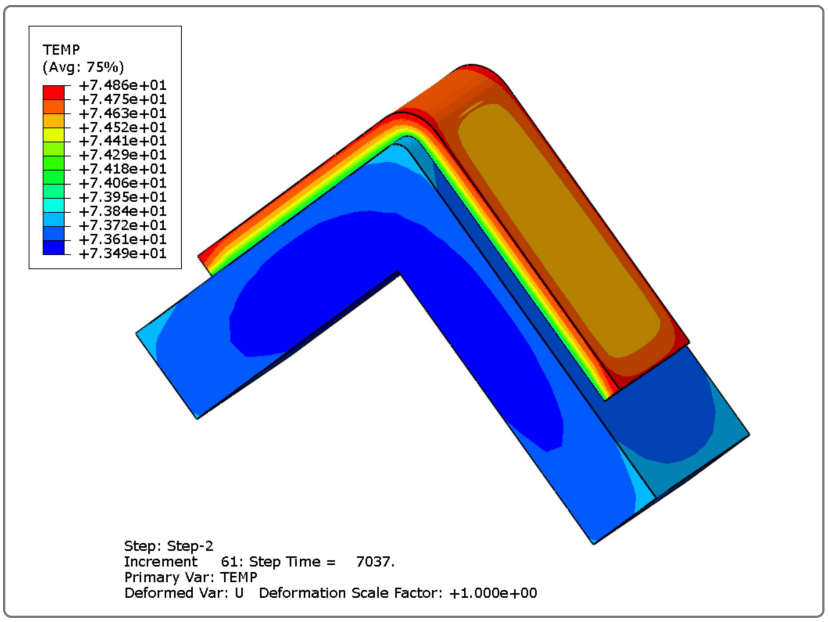

Figure 6. Temperature distribution of the bracket and tool assembly predicted by the sequentially coupled analysis.

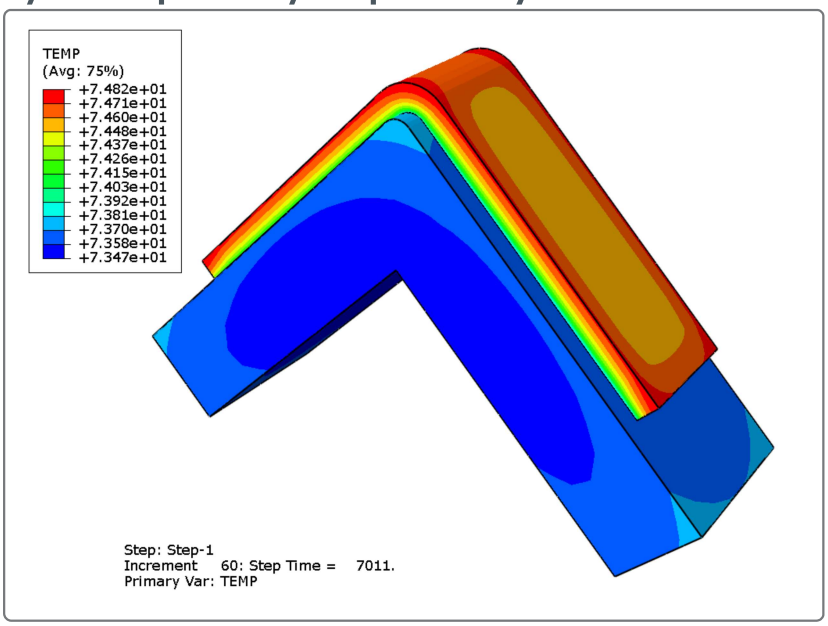

Figure 7. Shape distortion predicted by the fully coupled analysis (UD definition).

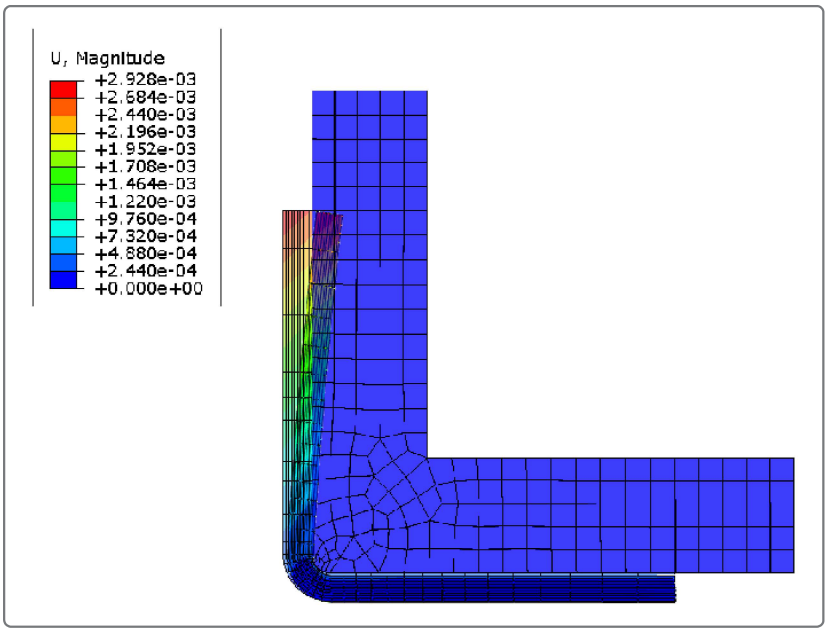

Figure 8. Shape distortion predicted by the sequentially coupled analysis (UD definition).

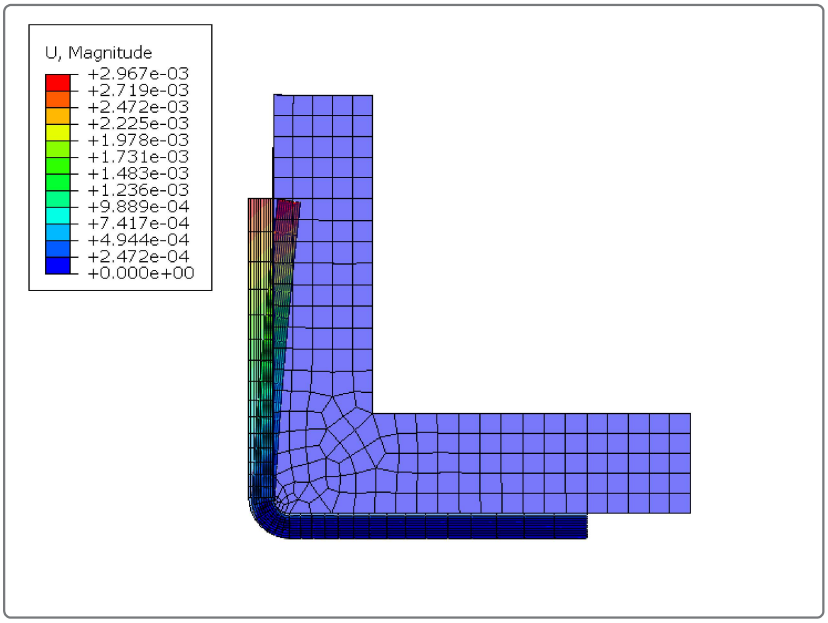

Figure 9. Shape distortion predicted by the fully coupled analysis (woven definition).

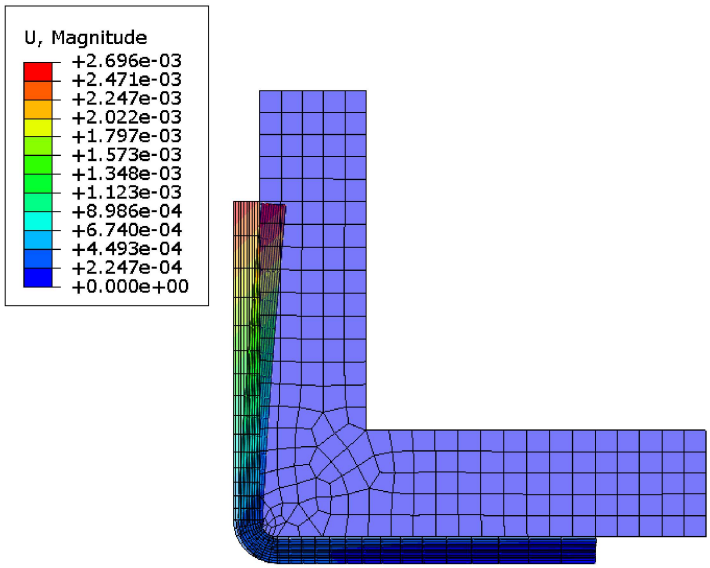

Figure 10. Displacement of the tip of the bracket.

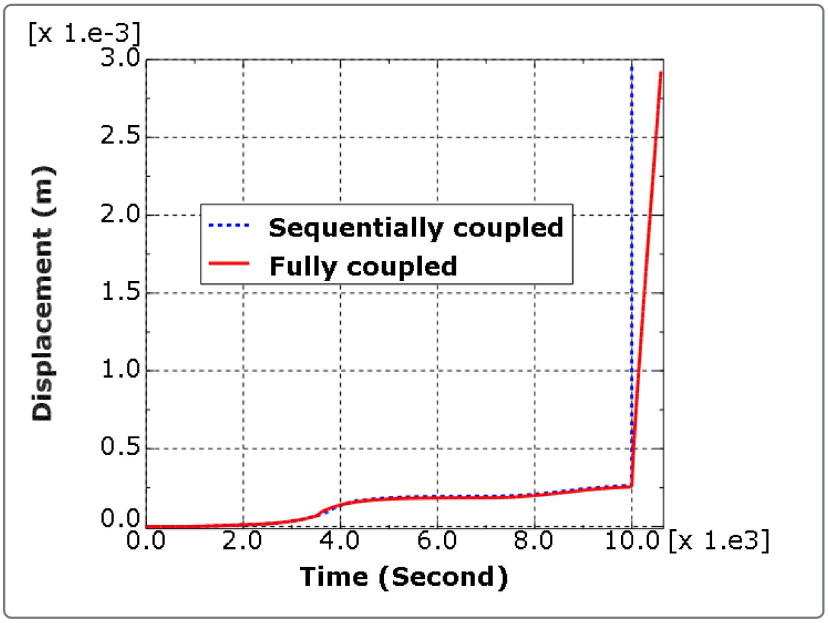

Figure 11. In-plane strains at element 4051.

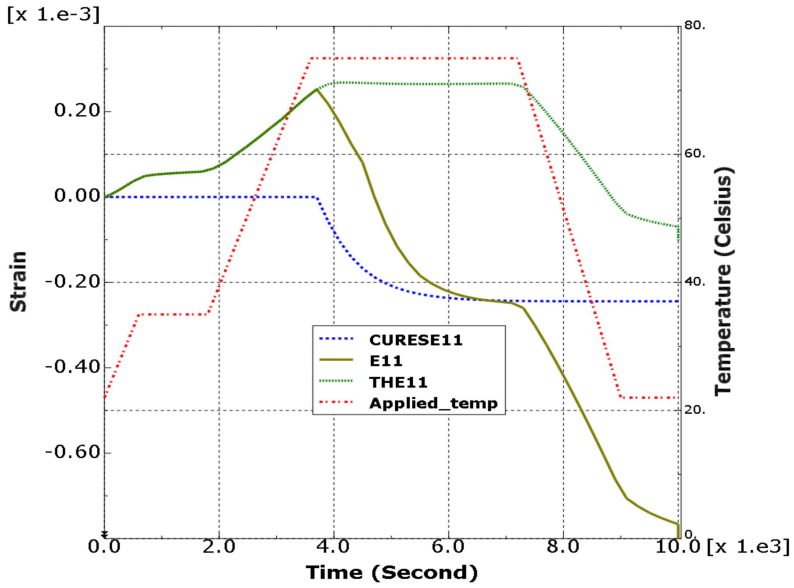

Figure 12. Out-of-plane strains at element 4051.

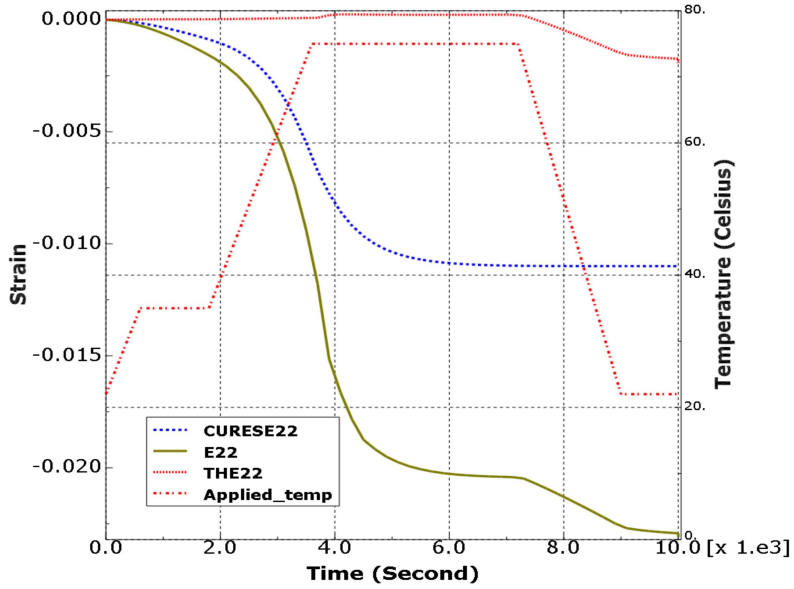

Figure 13. Residual stresses at element 3916.